E·MRS
EUROPEAN
MATERIALS RESEARCH SOCIETY

Strasbourg (France)

MANUSCRIPT COVER PAGE FORM

E-MRS Symposium : B - Material science issues in advanced CMOS source-drain engineering

Paper Number : 2049

Title of Paper : PHYSICALLY BASED MODELLING OF DAMAGE, AMORPHIZATION, AND RECRYSTALLIZATION FOR PREDICTIVE DEVICE-SIZE PROCESS SIMULATION

Corresponding Author : J.E. Rubio, M. Jaraiz, I. Martin-Bragado, R. Pinacho, P. Castrillo and J. Barbolla

Full Mailing Address : Dept. of Electronics, ETSI Telecomunicacion, University of Valladolid, 47011 Valladolid, SPAIN

Telephone : +34 983 423000 ext 5501

Fax : +34 983 423675

E-mail : jerg@ele.uva.es

PHYSICALLY BASED MODELLING OF DAMAGE, AMORPHIZATION, AND RECRYSTALLIZATION FOR PREDICTIVE DEVICE-SIZE PROCESS SIMULATION

J.E. Rubio, M. Jaraiz, I. Martin-Bragado, R. Pinacho, P. Castrillo and J. Barbolla, Dept. of Electronics, University of Valladolid, 47011 Valladolid, SPAIN

Current advanced CMOS source/drain engineering involves the use of amorphizing implants with 3D geometry. Upon annealing, the induced transient enhanced diffusion (TED) can only be accurately predicted if the amorphized region is correctly modeled, as well as the formation and evolution of extended defects, particularly 311's and dislocation loops. In addition to the extended defects, already modeled in the atomistic kinetic Monte Carlo simulator DADOS, we have developed a physically based modeling approach for the implant-induced damage build-up, amorphization and recrystallization, suitable to handle device-size process simulation. It is based on amorphous pockets (3D, irregular shape agglomerates of an arbitrary number of interstitials and vacancies, plus trapped impurities) with a size-dependent activation energy for recombination. The model is able to reproduce experimental aspects like the crystal-amorphous transition temperature and the super linear increase of damage with dose. We describe the model and present simulation examples. The efficiency of the model, in terms of CPU time and memory requirements, will also be discussed.

I. Introduction

Predictive modeling of state-of-the-art submicron device processing faces the challenge of having to deal with many different mechanisms that take place simultaneously, and that can not be neglected 'as a first approximation'. A representative example is a source/drain As implant and anneal [1]: it is not enough to have good models and parameters for As diffusion and clustering. Among other materials science issues, it is also necessary to be able to predict the extent of the amorphized region so that the number and size of the extended defects formed beyond the a/c interface upon recrystallization are correctly estimated. Even in that case, the time scale for TED will not be properly simulated until the ripening of the {311} defects and its transformation into dislocation loops has been achieved acceptably well. For low dose implants, on the other hand, interface trapping and segregation can also come into play.

As a part of this many-sided task, in this work we describe and present some examples of a physically based and computationally efficient model for ion implantation damage build up, that provides accurate predictions of some materials science properties related to amorphization (like temperature, dose rate and ion mass dependence) and still can handle up to full submicron device simulation size using just typical computer resources.

II. Model description

In this section we will describe the models that we are using for damage production and annealing in the DADOS [2] kinetic Monte Carlo simulator. DADOS gets from MARLOWE the coordinates of all the particles (interstitials, vacancies, and implanted impurity atoms) from each collision cascade. After reading a cascade, DADOS inserts

each of these particles sequentially in its simulation box. If there are no neighbors within the capture distance (second neighbors distance in Si) of a newly inserted particle, the particle remains as an isolated point defect (I, V) or impurity, referred hereinafter as an IP. If there is another IP within the capture distance the two are considered to form a new damage structure, called amorphous pocket or AP. Subsequent implanted particles will join this AP if they happen to fall within the capture radius of one of the constituent particles of the AP. Notice that the amorphous pocket particles are kept at their implanted coordinates, and thus the APs present irregular 3D shapes. In the simulation, if a newly formed AP overlaps with one or more already existing APs or IPs they are all merged and form a bigger AP. For simplicity, we will now assume only I and V particles and will discuss impurity atoms later on.

Heavier ions are known to produce denser cascades than light ions and consequently different damage morphology. Even the simple model described so far is able to capture this feature, as it can be seen from the comparison between the AP histograms (number of APs versus AP size, Fig. 1) for Si and Ge ions implanted into Si, for the same implant conditions of 80 keV energy and a dose rate of $5\cdot10^{12}$ $cm^{-2}s^{-1}$. The temperature was low enough to prevent dynamic annealing and allow for very effective damage accumulation. The dose, $4\cdot10^{12}$ cm^{-2}, was chosen below the amorphization threshold in both cases, to produce only APs. The heavier Ge ion produces larger APs than the Si ion, as reflected in the histograms of Fig. 1, where the AP size is taken as the number of IV pairs in it. This number is taken simply as the minimum of the number of Vs and Is in the AP, irrespective of their particular distance within it. If the total I+V particle count in the AP is used as AP size, instead of the number of IV pairs, the histograms exhibit the same trend, just adding a factor of two in the abscissa (not shown in Fig. 1). The IV pair was identified by theoretical calculations [3] as a metastable defect with a barrier for recombination. The agglomeration of multiple IV pairs [4] forms more stable

damage structures which exhibit an activation energy for recombination which lies between the recombination energy of the isolated IV pair (0.43 eV) and the recrystallization energy of the planar a/c Si interface (2.44 eV). Moreover, the agglomeration of multiple IV pairs to form amorphous pockets has been used to model amorphization and recrystallization in Si [5].

Our model for damage accumulation, amorphization and recrystallization [2] relies on the average statistical behavior of the damaged regions, instead of on the particular local configuration of each individual I or V particle. The aim of our approach was to be able to simulate full device size structures, which would require a prohibitive computer memory size if each IV pair had to be maintained in the simulation up to the amorphization threshold concentration. Until now we only dealt with room temperature implants. In this paper we present results after re-calibrating the AP parameters using variable temperature implant data to expand the range of applicability of the simulator. As it turns out, this simple model is enough to adequately reproduce the ion mass, temperature and dose rate dependence of Si amorphization in an efficient manner in terms of CPU time and memory usage up to submicron device size simulations.

Continuing with the description of our model, the AP activation energy for recombination is simply related to the number of IV pairs that it contains, irrespective of its particular spatial configuration. After recombining all its IV pairs, the AP can only dissolve through the emission of an I or a V point defect and has thus naturally become an I or V cluster, with its corresponding energy vs. size dependence. If the AP has also trapped impurities, then after recombining all its IV pairs it is split into small size impurity-point defect clusters (like As_nV_m, B_nI_m…) with low formation energy [1].

Overlapping APs can give rise to locally amorphized regions and, finally, to a continuous amorphous layer, during the implant. Once this layer (or arbitrary shaped region) has been amorphized, recrystallization is its only possible event. This process is

implemented by converting back amorphous boxes (of about 1 nm^3) to crystalline at a velocity that is thermally activated with an energy of 2.4 eV, and depositing any impurity atoms that it contains as an IP (up to the electrical solubility limit in the case of dopants) or in small impurity-point defect clusters, or sweeping a fraction of them with the recrystallization front. Next we describe the AP parameter calibration procedure and discuss some simulation results.

III. Results

Figure 2a represents the simulated relative damage level (I+V cm^{-3}) reached after an 80 keV, 10^{15} cm^{-2} Si implant, at different dose rates, versus implant temperature. These curves are similar to the ones obtained from RBS measurements by Schultz et al. [6] at 1 MeV implant energy. Fig. 2b is the corresponding Arrhenius plot and, in addition to the data points from Schultz's measurements, includes the 80 keV experimental data obtained by Goldberg et al. [7], who determined the temperature at which an amorphous layer first appears when silicon is irradiated with ions ranging in mass from 12 (C) to 132 amu (Xe). The apparent activation energies determined from the data span from 0.7 to 1.7 eV and increase as a function of ion mass. They found that the activation energy for silicon was 0.84 eV. We have used Goldberg's data for calibrating the AP recombination energy as a function of the AP size (IV number), assigning 0.5 eV to the size one AP. A good fit is obtained for the whole temperature/dose rate range, as it can be seen in Fig. 2b.

Figure 3 plots the contribution of the different damage and defect structures present in the material versus temperature. At the low temperatures there is a continuous amorphous layer at the damage peak, surrounded by highly damaged but not yet amorphized regions containing APs. At the high temperature end, only clusters are

stable enough to be seen. An increase in dose rate yields curves similar to these ones, only shifted to higher temperatures.

Figure 4 shows the damage composition versus implanted dose for a Si implant (a) and for a Ge implant (b) at low temperature, at the same dose rate, up to a dose enough to amorphize in both cases. The onset of amorphization takes place at a lower dose for Ge than for Si, as expected. Notice the super linear behavior of the (total) accumulated damage vs. dose.

Finally, as stated before, the purpose of our model was to be able to drastically cut down computer CPU and memory requirements by not having to keep track of each and every I, V generated by the cascades up to the amorphization damage level, that is, beyond 10^{22} cm^{-3}. Since the recombination rate of our APs is based not on local configuration but on their 'size' (IV count) we have added the following approach to reduce memory usage without sensibly affecting the simulation. I and V particles are incorporated into the DADOS simulation box until a certain concentration level, e.g. 10^{20} cm^{-3}, is reached. Beyond that level, particles in APs are 'hidden' randomly, but the AP maintains a count of its numbers of Is and Vs as it captures new particles or recombines some of its IV pairs. As we show below, this simple maintenance task suffices to preserve the correct recombination rate of the APs. At the same time, a particle concentration around 10^{20} cm^{-3} also seems to provide a number of AP 'representative' particles (present in the simulation box) that is enough to capture as much as necessary of the newly implanted I and V particles to yield the correct simulation result. This can be seen in the comparison shown in Figure 5 between a simulation run without limiting the particle concentration up to amorphization (a) and limiting the particle concentration in the simulation box at a level of 10^{20} cm^{-3}, that is, more than two orders of magnitude below, and yet the model still predicts almost the same damage composition and evolution.

IV. Conclusions

We have shown that it is possible to model damage accumulation up to amorphization in the kinetic Monte Carlo method, with a number of particles kept in the simulation at least two orders of magnitude less than the actual amorphization level. In spite of this drastic reduction in computer memory and CPU requirements, the model accurately predicts the temperature and dose rate dependence and reveals different damage structure depending on the ion mass. Further work is underway to calibrate it for different ion masses. This model can be used to simulate amorphization conditions up to full submicron device size structures.

REFERENCES

1. R. Pinacho, M. Jaraiz, P. Castrillo, J.E. Rubio, I. Martin-Bragado and J. Barbolla, accepted in EMRS-04, symposium B
2. M. Jaraiz, P. Castrillo, R. Pinacho, I. Martin-Bragado and J. Barbolla, in D. Tsoukalas and C. Tsamis (Eds), Simulation of Semiconductor Processes and Devices 2001, 2001, p. 10.
3. M. Tang, L. Colombo, J. Zhu and T. Diaz de la Rubia, Phys. Rev. B, 55 (1997) 14279.
4. L. A. Marques, L. Pelaz, M. Aboy, L. Enriquez and J. Barbolla, Phys. Rev. B, 91 (2003) 135504-1.
5. L. Pelaz, L.A. Marqués, M. Aboy, J. Barbolla and G. H. Gilmer, Appl. Phys. Lett., 82 (2003) 2038.
6. P. J. Schultz, C. Jagadish, M. C. Ridgeway and R. G. Elliman, and J. S. Williams, Phys. Rev. B, 44 (1991) 9118.
7. R.D. Goldberg, J.S. Williams and R.G. Elliman, Nucl. Instrum. Methods Phys. Res. B, 106 (1995) 242.

FIGURE CAPTIONS

Fig. 1. Amorphous pockets histograms for 80 keV Si and Ge ions implanted at -200 °C to a dose of $4\cdot10^{12}$ cm^{-2} (sub-amorphizing) at a dose rate of $5\cdot10^{12}$ $cm^{-2}s^{-1}$.

Fig. 2. (a) Calculated damage vs. substrate temperature for 80 keV, 10^{15} cm^{-2} Si implants at dose rates ranging from $2\cdot10^{11}$ $cm^{-2}s^{-1}$ to $5\cdot10^{13}$ $cm^{-2}s^{-1}$. (b) Crystalline-amorphous transition temperature as a function of dose rate. Solid squares correspond to the simulations in (a). Stars and open triangles correspond to experiments at energies of 80 keV [7] and 1 MeV [6], respectively.

Fig. 3. Contribution of different defect structures to the total damage for an 80 keV, 10^{15} cm^{-2} Si implant at a dose rate of $2\cdot10^{11}$ $cm^{-2}s^{-1}$, as a function of the substrate temperature.

Fig. 4. Dose dependence of the damage fraction due to different defect structures for 80 keV Si (a) and Ge (b) implants at a dose rate of $5\cdot10^{12}$ $cm^{-2}s^{-1}$ and a temperature of -20 °C.

Fig. 5. (a) and (b) represent the dose dependence of the damage fraction due to different defects for an 80 keV Si implant at a temperature of 70 °C and a dose rate of $5\cdot10^{12}$ $cm^{-2}s^{-1}$. For comparison, in the simulation (a) there is no concentration limit while in the simulation (b) the maximum particle concentration in the simulation box is limited to 10^{20} cm^{-3} to save computer resources.

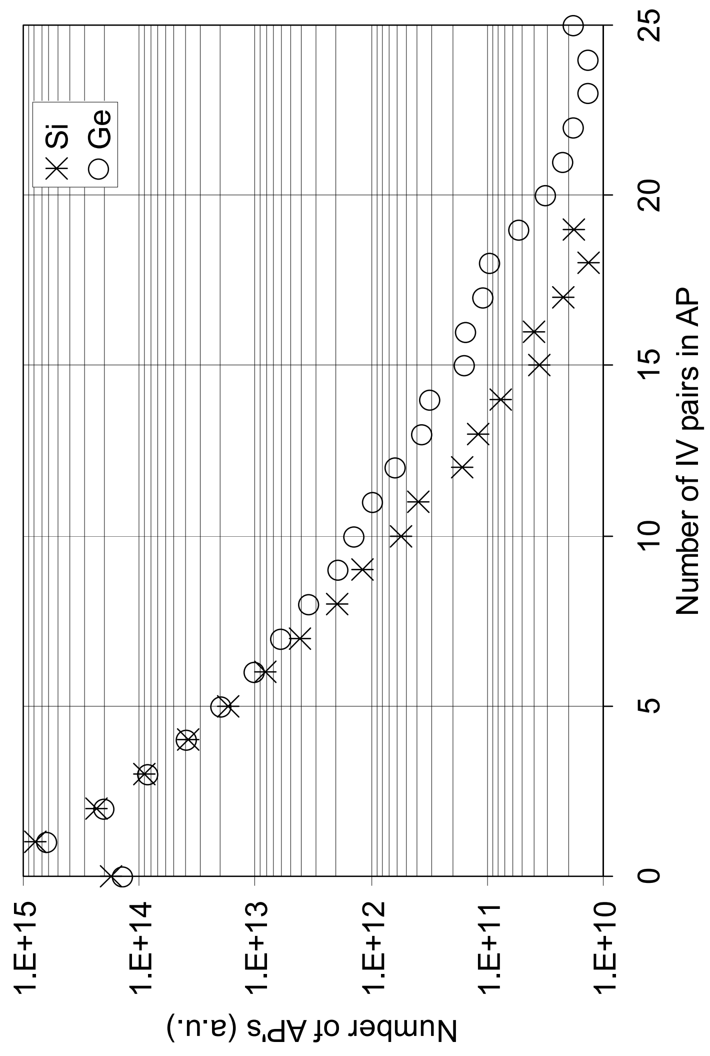

Fig. 1

(a)

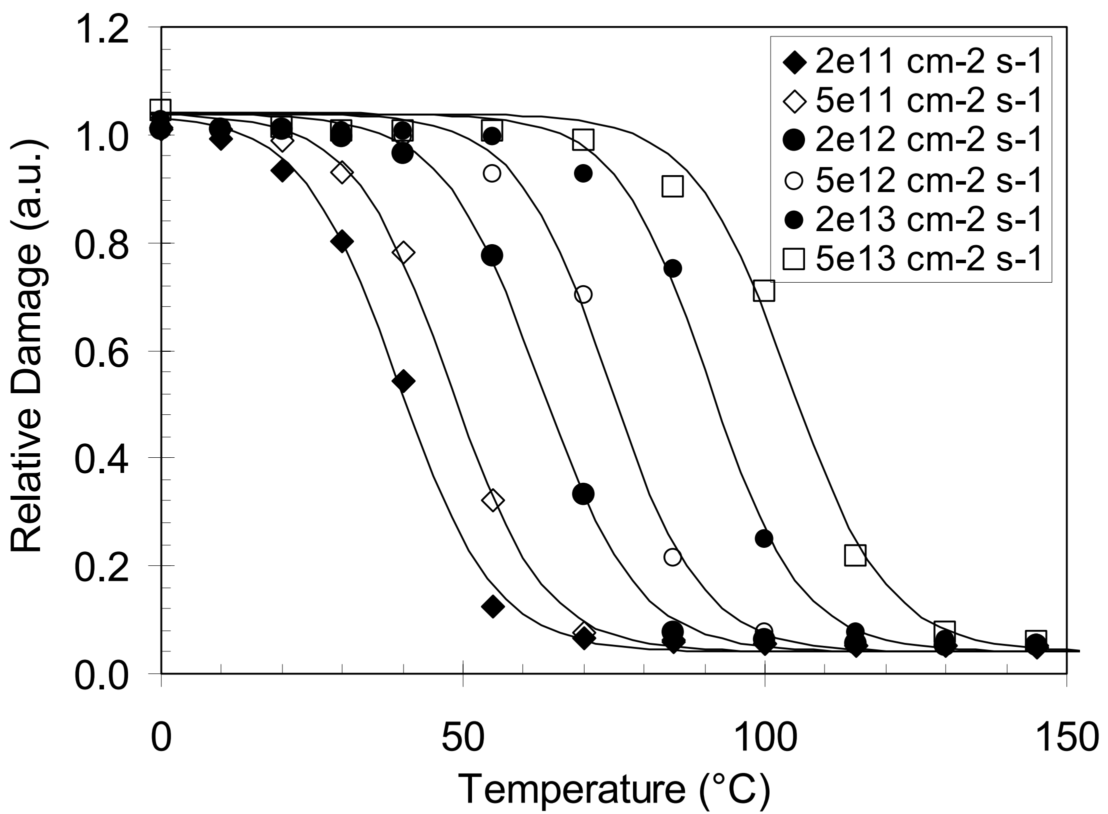

Fig. 2 a

(b)

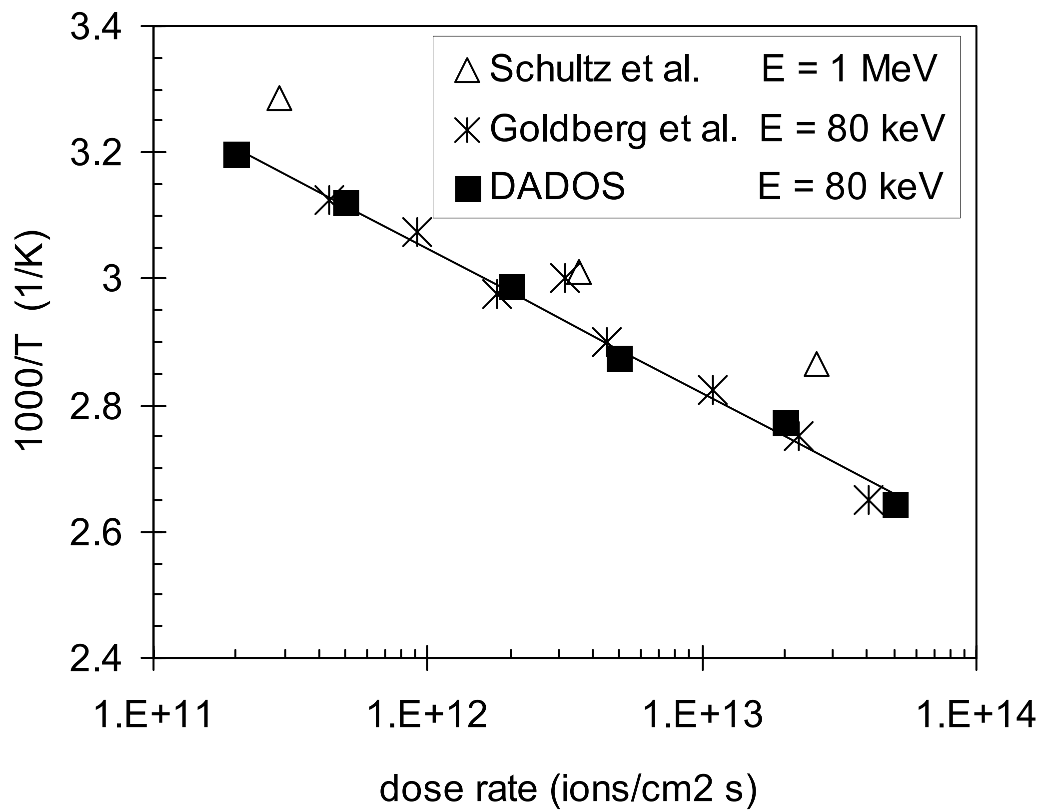

Fig. 2 b

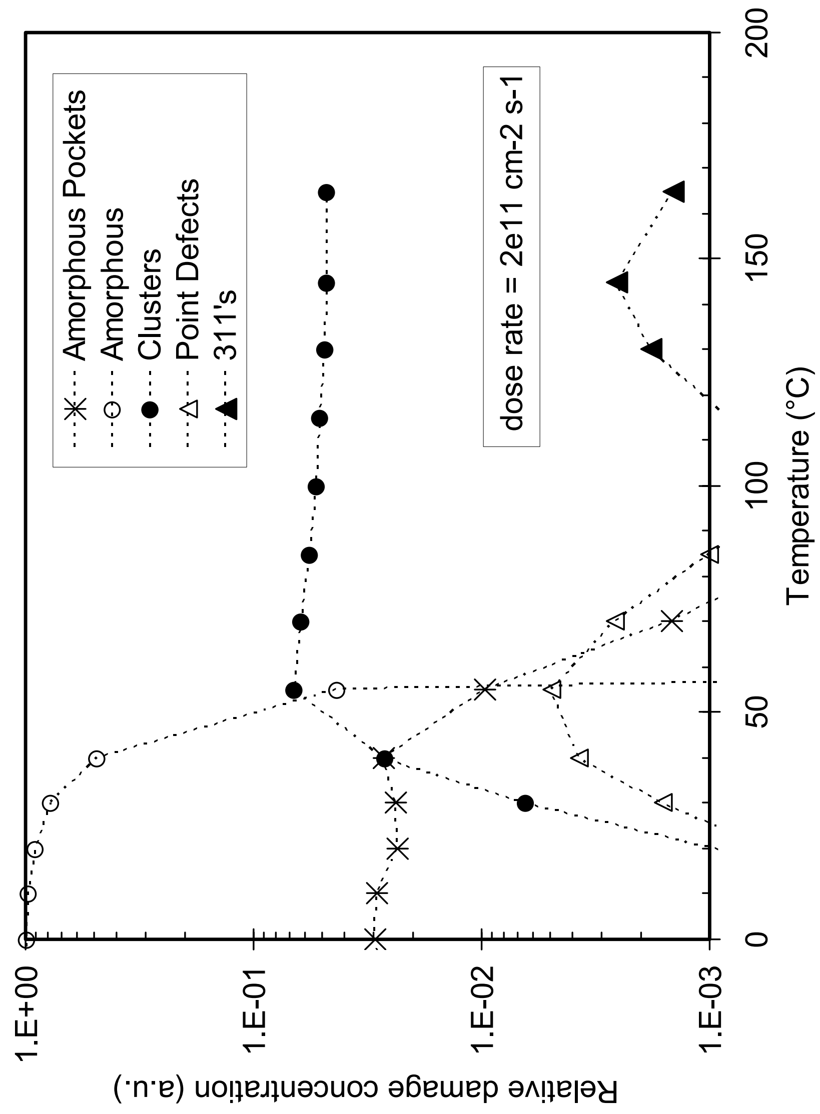

Fig. 3

(a)

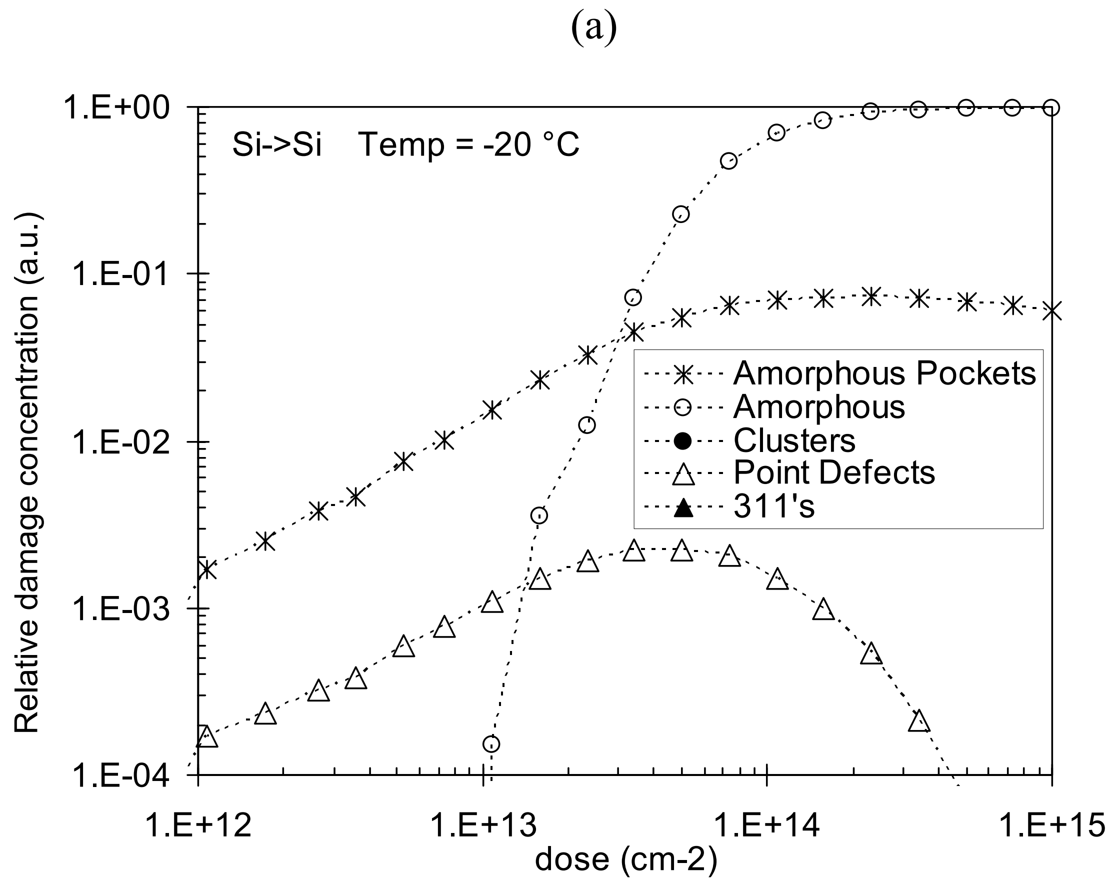

Fig. 4 a

(b)

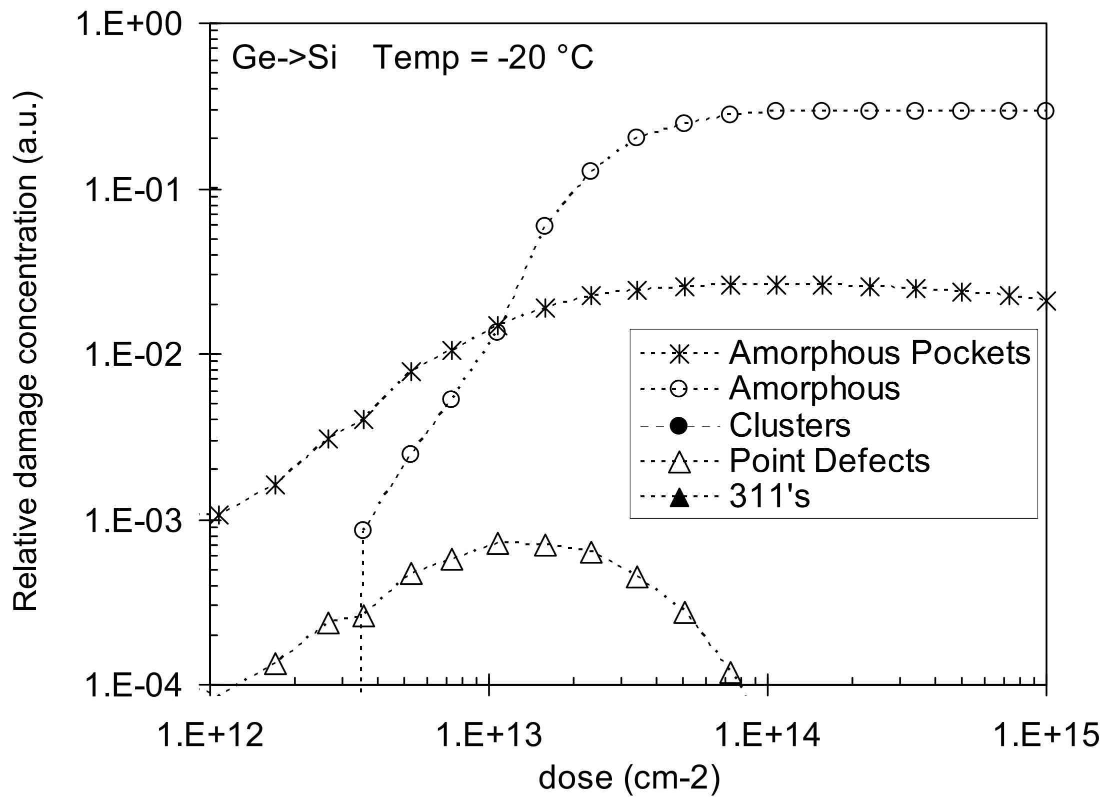

Fig. 4 b

(a)

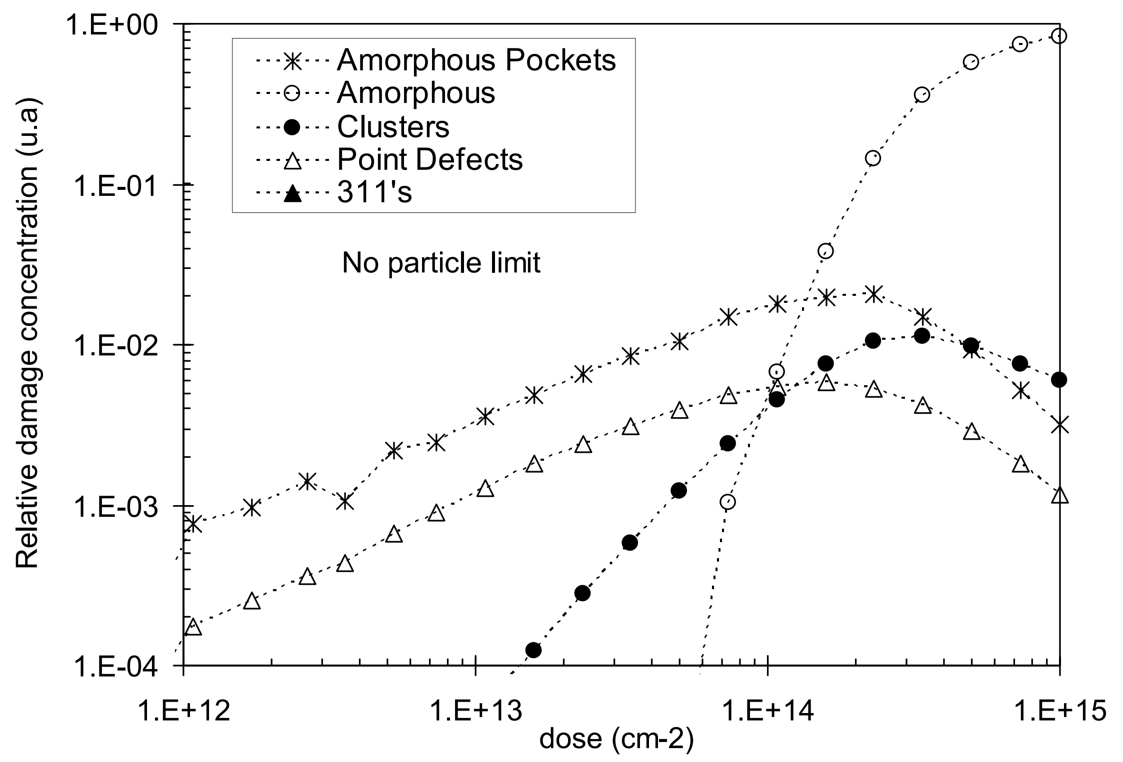

Fig. 5 a

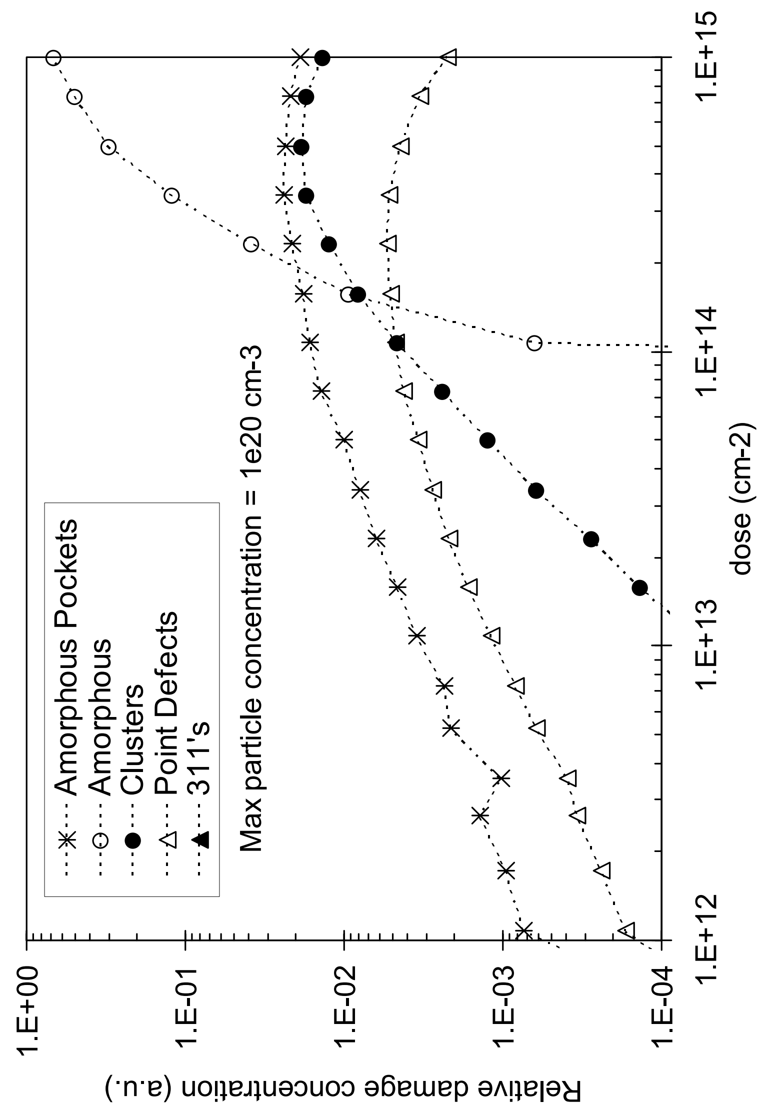

Fig. 5 b